WILEY InterScience® DISCOVER SOMETHING GREAT

PROTEINS STRUCTURE ■ FUNCTION ■ BIOINFORMATICS

Identification of fungal oxaloacetate hydrolyase within the isocitrate lyase/PEP mutase enzyme superfamily using a sequence marker-based method

Henk-Jan Joosten,[1] Ying Han,[2] Weiling Niu,[2] Jacques Vervoort,[3] Debra Dunaway-Mariano,[2] and Peter J. Schaap[1]*

[1] Laboratory of Microbiology, Wageningen University, 6703 HA Wageningen, The Netherlands
[2] Department of Chemistry, University of New Mexico, Albuquerque, New Mexico 87131
[3] Laboratory Biochemistry, Wageningen University, 6703 HA Wageningen, The Netherlands

ABSTRACT

Aspergillus niger** produces oxalic acid through the hydrolysis of oxaloacetate, catalyzed by the cytoplasmic enzyme oxaloacetate acetylhydrolase (OAH). The **A. niger** genome encodes four additional open reading frames with strong sequence similarity to OAH yet only the **oahA** gene encodes OAH activity. OAH and OAH-like proteins form subclass of the isocitrate lyase/PEP mutase enzyme superfamily, which is ubiquitous present filamentous fungi. Analysis of function-specific residues using a superfamily-based approach revealed an active site serine as a possible sequence marker for OAH activity. We propose that presence of this serine in family members correlates with presence of OAH activity whereas its absence correlates with absence of OAH. This hypothesis was tested by carrying out a serine mutagenesis study with the OAH from the fungal oxalic acid producer **Botrytis cinerea** and the OAH active plant petal death protein as test systems.

Proteins 2008; 70:157–166.

***Key words:** multiple protein structural alignment; family-based approach; **Aspergillus niger**; **Botrytis cinerea**; plant petal death protein; lyase; gem-diol.*

INTRODUCTION

Filamentous fungi, such as the food biotechnology fungus *Aspergillus niger*, the opportunistic human pathogen *A. fumigatus*, the phytopathogenic fungi *Botrytis cinerea* and *Sclerotinia sclerotiorum*, and numerous brown-rot and white-rot basidiomycetes are able to efficiently produce and secrete large quantities of oxalate.[1] Because oxalate is toxic (a concern in using fungi for commercial food and drug production) and a key factor in fungal pathogenesis,[2–5] it is important to distinguish oxalate-producing strains from nonproducing strains. Oxalate can be formed from oxaloacetate in a C—C bond lysis reaction catalyzed by oxaloacetate hydrolase (oxaloacetate acetylhydrolase, OAH, EC 3.7.1.1)[6] and from the oxidation of glyoxylate[7] and glycolaldehyde.[8] The acetoacetate/OAH route predominates in oxalate producers examined to date[1,9–14] and therefore the *oah* gene might be used for the classification of fungi as potential oxalate producers.

Recently, the genomes of a large number of oxalate and nonoxalate producing fungi have been sequenced. The object of this work was to correlate the ability of fungi to produce oxalate with the presence of an *oah* gene in their genome. This task was made difficult by the fact that fungal genomes encode several OAH homologs having an unusually high level of shared sequence identity. Thus, identification of OAH activity in the gene product would require purification of each protein followed by *in vitro* OAH activity testing. A less time consuming approach, based on structure-function analysis of OAH was therefore pursued. In this article we propose the identification of a sequence marker for OAH activity that can be used to identify the *oah* gene in fungal genomes.

Family-based approaches that combine 3D structure data with sequence analyses techniques are powerful methods to reveal the function of residues.[15] To identify OAH specific sequence markers this approach was applied to isocitrate lyase/PEP mutase superfamily of which OAH is a member. A large structure-based superfamily multiple sequence alignment (3D-MSA) was built to which we have applied a general numbering scheme (3D-numbers) for structurally

The Supplementary Material referred to in this article can be found online at http://www.interscience.wiley.com/jpages/0887-3585/suppmat.
Grant sponsor: NIH; Grant number: GM28688; Grant sponsor: VLAG Graduate School.
Henk-Jan Joosten and Ying Han contributed equally to this work.
*Correspondence to: Peter J. Schaap, Laboratory of Microbiology, Dreijenlaan 2, 6703 HA Wageningen, The Netherlands. E-mail: peter.schaap@wur.nl
Received 7 December 2006; Revised 4 April 2007; Accepted 26 April 2007
Published online 24 July 2007 in Wiley InterScience (www.interscience.wiley.com). DOI: 10.1002/prot.21622

conserved positions. This 3D-numbering scheme will be used throughout this article. From this structural alignment we were able to segregate sequences into subclasses, one of which we named the OAH-like class of fungal proteins. The sequences of the members of this subclass from fungi with confirmed OAH activity[12,16–19] were shown to be distinguished by the presence of a serine, which from homology modeling and comparison to the recently reported structure of the OAH active plant petal death protein, we know to be located within the active site. By carrying out amino acid replacement experiments with recombinant OAH from *Botrytis cinerea* and with the recombinant OAH-active petal death protein from *Dianthus caryophyllus* (carnation),[20] we tested the contribution that the active site serine makes in catalysis of OAH cleavage. Here we report the results from these studies which support the role of the active site serine in OAH catalysis, and which provide insight into the divergence of OAH activity within the α-hydroxyacid C—C lyase branch of the isocitrate lysase/PEP mutase enzyme superfamily. Moreover, we show that the active site serine identified by analyses of the 3D-MSA is a reliable sequence marker for OAH activity.

METHODS

Enzymes

Recombinant *Botrytis cinerea* OAH and *Dianthus caryophyllus* petal death protein were prepared according to published procedure.[20,21] Site-directed mutants were prepared using a PCR-based strategy with *pfu* polymerase. The plasmids OAH-pET-3c and petal death protein-Pet-3c served as template in conjunction with commercial custom primers. Gene sequences were verified by nucleotide sequencing. The mutant proteins were purified to homogeneity (as judged by SDS-PAGE analysis; supplementary file) using the same protocol reported for the purification of the wild-type enzymes.[20,21] The mutant proteins behaved chromatographically the same as the wild-type enzymes and were stable upon storage.

Activity assays

The conversion of oxaloacetate to oxalate and acetate was monitored using the assay as reported.[20] The lysis reactions of (3S, 2R) 2-ethyl-3-methylmalate and (3S, 2R) 2,3-dimethylmalate were monitored as described previously.[20]

Steady-state kinetic constant determination

The steady-state kinetic parameters (K_m gem and k_{cat}) for reactions catalyzed by OAH and the petal death protein were determined from the initial velocity data measured as a function of substrate concentrations. The initial velocity data were fitted to Eq. (1) with KinetAsystI

$$V_0 = V_{max}[S]/(K_m + [S]) \quad (1)$$

where [S] is the substrate concentration, V_0 is the initial velocity, V_{max} is the maximum velocity, and K_m is the Michaelis–Menten constant for the substrate. The k_{cat} value was calculated from V_{max} and the enzyme concentration using the equation $k_{cat} = V_{max}/[E]$, where [E] is the protein subunit molar concentration.

Data collection, creation, and screening of the 3D-MSA

The isocitrate lyase/PEP mutase enzyme superfamily protein structures were collected from the Structural Classification of Proteins (SCOP)[22] structure comparison resource. The superfamilly sequences were collected by BLAST searches using the sequences of the structures as queries. To collect all closely related fungal proteins from the 18 annotated publicly available fungal genomes BLAST searches were performed in the corresponding protein sets. To find additional OAH-like proteins BLAST searches were performed in the Concordia EST collection database (https://fungalgenomics.concordia.ca/). The 17 structure files of the superfamily were divided into subfamilies according to SCOP. Structure superposition and sequence alignment were performed using WHATIF.[23] The complete superfamily alignment was built as described.[15] The alignment was used for correlated mutation analyses (CMA) using a CMA-score algorithm based on the method described by Shulman et al.[24] Details of the algorithm can be found at our website (http://3dmscis.systemsbiology.nl). OAH specific amino acids were identified by scanning the alignment for positions that are 100% conserved in all OAHs and a different residue in the rest of the alignment. Different is here defined as present in less than 5% of the remaining sequences.

Fungal phylogenetic tree

Twelve fungal panorthologous genes were selected and the protein sequences were aligned using clustalW.[25] Alignments were manually curated for ambiguous aligned sequences and concatenated. Maximum likelyhood phylogenetic analysis was carried out with Tree Puzzle[26] using the VT model[27] and a gamma model of rate heterogeneity with alpha = 0.64.

Distance tree

A neighbor joining tree was built of all collected proteins belonging to the OAH-like protein class, together with CPPM from *S. hygroscopicus* and the putative methyl

DOI 10.1002/prot

isocitrate lyase (MICL) proteins from all 17 completely sequenced fungi functionally related diversification residues used in this study. Only the structurally conserved regions were used as aligned input for QuickTree[28] to build the tree. The tree was visualized with Treeview.[29]

Analysis of synteny

Two ORFs directly adjacent to ORFs encoding OAH-like class proteins were used to query fungal genomes encoding one or more OAH-like class proteins by blastX and if a single very highly significant hit resulted (*E*-value $< 1\ E\ -10$), this was considered to be the likely ortholog of the query. When two genes were found to be adjacent in two different species, they were determined to be located in the same synteny segment in those species.

Modeling of gem-diol bound in the active site of PDP

1ZLP was used as template to create a structure of PDP with bound gem-diol of oxaloacetate. The gem-diol was created using the build option of YASARA followed by energy minimization (EM) using YASARAs YAMBER2 force field as described.[30] The resulting gem-diol was modeled in the active site of PDP by superimposing it on 5-hydroxypentanal: a compound covalently bound in the active site of PDP in structure 1ZLP. A hydroxyl group attached to C2 (Fig. 5) of the gem-diol was superimposed on the hydroxyl group of 5-hydroxypentanal. C2 and the next two carbons (R-group, Fig. 5) of the gem-diol were superimposed on the first three carbon atoms attached to the hydroxyl group of 5-hydroxypentanal. After superpositioning, the remaining hydroxyl group attached to C2 in the gem-diol was optimally positioned for hydrogen bond formation with S157 (3D-numbering scheme) (Fig. 5B).

RESULTS AND DISCUSSION

Identification of the fungal OAH and OAH-like subclass of the isocitrate lyase/PEP mutase enzyme superfamily

The *Aspergillus niger* OAH protein sequence was used in BLAST[16] searches for the identification of similar

Table I
OAH-Like Class Proteins in 25 Fungal Proteomes

Species	Source (db)[a]	Abbr.	Protein Acc. No.	Taxonomy
Ascomycota (complete sequenced genomes with predicted proteomes)				
Saccharomyces cerevisiae	1	Sce	–	Saccharomycotina
Kluyveromyces lactis	1	Kla	–	
Ashbya gossypii	1	Ago	–	
Debaryomyces hansenii	1	Dha	–	
Candida albicans	1	Can	–	
Yarrowia lipolytica	1	Yli	–	
Schizosaccharomyces pombe	1	Spo	–	Taphrinomycotina
Neurospora crassa	1	Ncr	XP-322273	Sordariomycetes
Magnaporthe grisea	1	Mgi	–	
Gibberella zeae	1	Gze	XP_391313	
Chaetomium globosum	2	Cgl	–	
Trichoderma reesie	3	Tre	33777	
Aspergillus nidulans	1	Ani	XP_661409, XP_664486, XP_682638	Eurotiomycetes
Aspergillus fumigatus	1	Afu	**EAL87152**, EAL87476, XP_746468, EAL87110	
Aspergillus niger	1	Ang	**CAD99195**, ABC73717, ABC73718, ABC73719, ABC73720	
Aspergillus oryzae	1	Aor	**BAE62045**, BAE56423, BAE66408, BAE62647, BAE60526	
Stagonospora nodorum	2	Sno	SNU10723	Dothideomycetes
Botrytis cinerea	2	Bci	**AAS99938**	Leotiomycetes
			BC1G01599	
Sclerotinia sclerotiorum	2	Ssc	**SS1G_08218**	
Basidiomycota (complete genomes with predicted proteomes)				
Cryptococcus neoformans	3	Cne	–	Hymenomycetes
Phanerochaete chrysosporium	3	Pch	**7156**	
			7400	
Coprinus cinereus	2	Cci	**CC1G_06900.1**	
Ustilago maydis	1	Uma	EAK82071	Ustilaginomycetes
Basidiomycota (other)				
Gloeophyllum trabeum	4	Tra	tra_1, tra_2	
Ceriporiopsis subvermispora	5	Cvs	**Cvs_OAH**	

Known oxalate producers and (putative) OAH are in bold. BLAST searches were done with an expectation limit $< 1\ e\ -5$.
[a]Complete proteomes and individual sequences were retrieved from the following on line databases 1: NR-database, www.ncbi.nlm.nih.gov/; 2: Broad institute, www.broad.mit.edu/; 3: Joint Genome Institute, www.jgi.doe.gov/; 4 Concordia EST collection, https://fungalgenomics.concordia.ca/; 5: Sequence extracted from US Patent 6939701.

sequences within the *A. niger* predicted proteome, in the nonredundant (NR) protein database using the default settings, and in predicted proteomes of completely sequenced fungal genomes. The results are summarized in Table I. Most of the queried filamentous fungal genomes have one or more genes which appear to encode OAH-like proteins and have strong sequence similarity to the *A. niger oahA* gene (Table I) (Fig. 1).

On the basis of the BLAST searches performed using the NCBI NR database, we found that the corresponding fungal proteins belong to the isocitrate lyase/PEP mutase enzyme superfamily. The closest sequence homolog to the OAH and OAH-like proteins is the carboxyvinyl-carboxyphosphonate phosphorylmutase (CPPM, EC 2.7.8.23) of the gram-positive bacterium *Streptomyces hygroscopicus*. The closest related subclass in fungi is the methyl isocitrate lyase (MICL) subfamily present in all fungi including yeasts (Fig. 2). A third subclass of closely related proteins is represented by the *Dianthus caryophyllus* (carnation) petal death protein (PDP).[31] This enzyme catalyzes the hydrolytic cleavage of oxaloacetate to oxalate and acetate as well as the C—C bond lysis of 2R-alkyl-malates.[20]

Using the method of Folkertsma et al.[15] a 3D-MSA of the isocitrate lyase/PEP mutase superfamily proteins was generated including all amino acid sequences from all translated orthologous and paralogous genes encoding fungal OAH-like class genes. Six most evolutionary distantly related sequences among the 18 reported X-ray structures representing the superfamily were used as starting sequences to build the alignment. These structures are isocitrate lyase (1DQU) from the fungus *Aspergillus nidulans*, two bacterial isocitrate lyases (1F61 and 1IGW), methyl isocitrate lyase (1MUM) of *Escherichia coli*, mollusk phosphoenolpyruvate phosphomutase (1PYM) and the petal death protein of *Dianthus caryophyllus* (1ZLP). The OAH-like class of fungal proteins were aligned using a profile derived from the petal death protein structure. The complete 3D-MSA can be retrieved from our website (http://fungen.wur.nl/OAH).

The 3D-MSA was used to construct a distance tree of OAH and OAH-like fungal proteins together with the carboxyPEP mutase of *S. hygroscopicus, the* PDP of *D. caryophyllus* and the fungal 2-methylisocitrate lyases (Fig. 2). This distance tree shows a strong clustering of the OAH proteins of *A. niger* and *B. cinerea* (both organisms are confirmed oxalate producers[12,16]) with putative protein EAL87152 of *A. fumigatus*, putative protein BAE62045 from *Aspergillus oryzae* and putative protein SS1G.08218 of *Sclerotinia sclerotiorum*. *A. fumigatus*,[17] and *S. sclerotiorum*[18] are also known oxalate producers. The clustering suggests that the latter three fungal genomes, as well as that of the *A. oryzae* genome, encode OAH.

In contrast, *A. nidulans* is not an oxalate producer. Consistent with this fact is the finding that although the *A. nidulans* genome contains three OAH-like genes, the

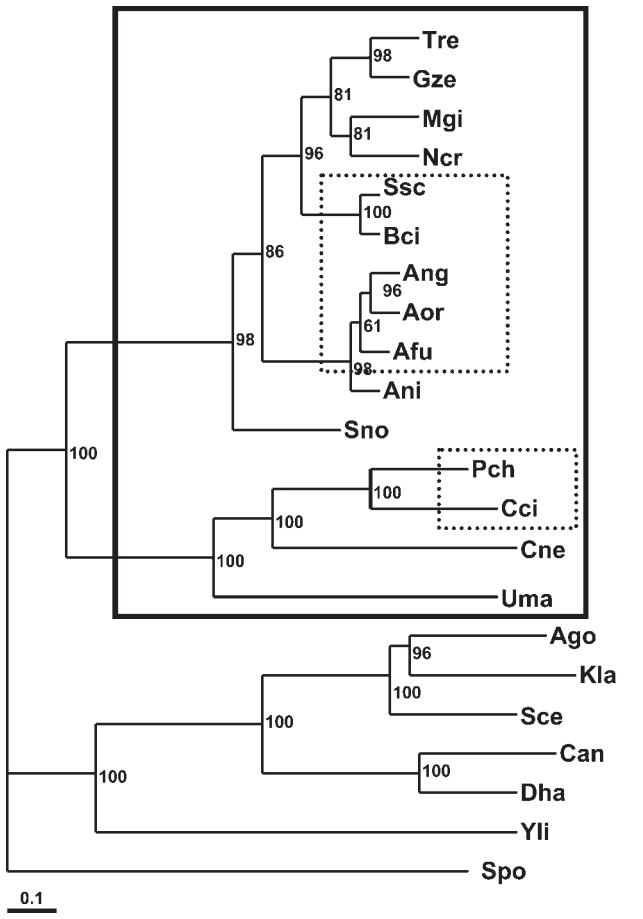

Figure 1

Maximum likelihood phylogenetic tree of 22 completely sequenced fungi. Fungal genomes encoding OAH-like class proteins are enclosed by a rectangle with a solid border. Rectangles with dotted borders enclose genomes encoding a (putative) OAH. For species abbreviations see Table I.

distance tree analysis suggests that none of these three genes encode OAH. This conclusion is also supported by the genome contexts in which the three OAH-like genes are found. Specifically, we screened all reported fungal genomes for possible conservation of synteny at the respective loci. Conservation of gene order was detected in the regions flanking the genes encoding the OAH of *A. niger* OAH and *B. cinerea*, and the genes encoding the putative OAHs EAL87152 of *A. fumigatus*, BAE62045 of *A. oryzae* and SS1G.08218 of *S. sclerotiorum* (Fig. 3 panel A). Conservation of gene order was also detected for the regions flanking the genes encoding the closest related paralogs of OAH, protein DQ349131 of *A. niger*, XP_661409 of *A. nidulans* and EAL87476 of *A. fumigatus* (Fig. 3 panel B). Finally, we observed conservation of gene order in the regions flanking the genes encoding the OAH-like proteins DQ349134 of *A. niger*, EAL87110 of *A. fumigatus* and XP_664486 of *A. nidulans* (Fig. 3 panel C). Detection of conservation of gene order at these three

DOI 10.1002/prot

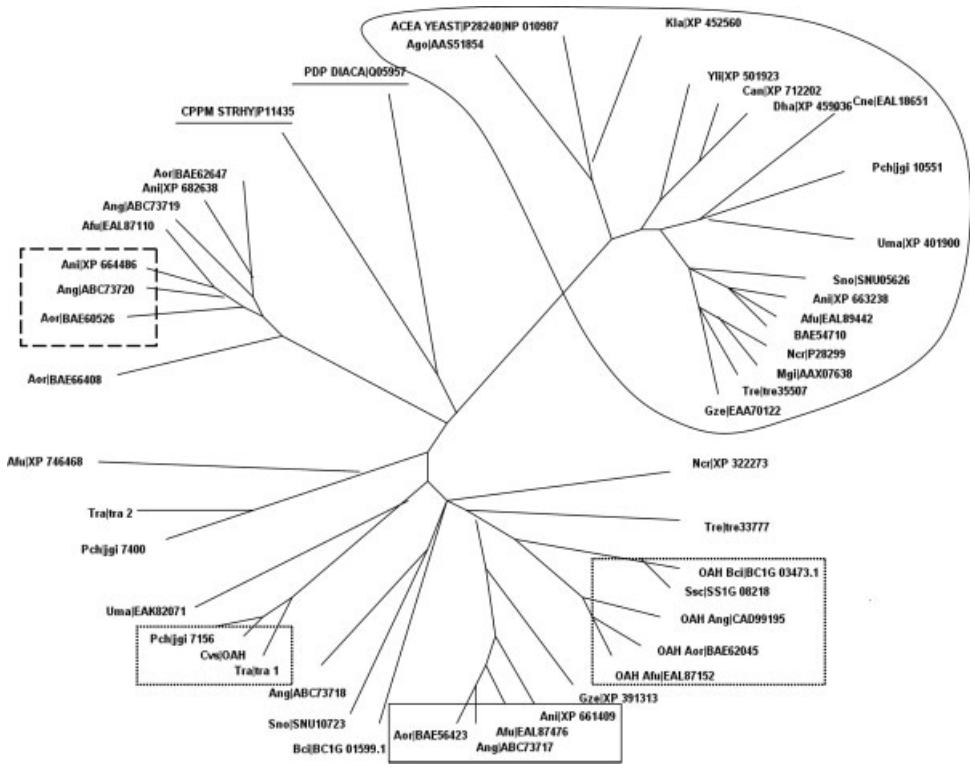

Figure 2

Distance tree of the OAH-like protein class, CPPM of Streptomyces hygroscopicus, Dianthus caryophyllus *PDP (PDP_IDACA) and putative fungal MICL proteins (enclosed in solid border). Rectangles enclose different orthologous groups of OAH-like class proteins. Dotted borders enclose (putative) OAH. Solid and dashed borders enclose two different orthologous groups of OAH-like class proteins.*

loci suggests that within *Aspergilli* there are at least three clusters of orthologous groups of OAH-like proteins. No further conservation of gene order was found surrounding any other OAH class protein of any of the other fungi.

Multiple, closely related genes encoding OAH class proteins were found in the completed basidiomycete fungal genomes. The whiterot fungus *Phanerochaete chrysosporium* is an oxalate producer.[19] The genome encodes two OAH-like class proteins (Table I). The closest homolog of the *C. subvermispora* OAH protein is ORF 7156 suggesting that this putative *P. chrysosporium* protein is in fact OAH (Fig. 2). In addition, we detected a probable OAH encoding gene in the inferred proteome of *Coprinus cinereus* (Table I) (Fig. 2), and we could assemble from an EST sequence library from the brown-rot basidiomycete *Gloeophyllum trabeum* two unigenes encoding OAH-like class proteins. One of these is very similar (76% sequence identity) to the *C. subvermispora* OAH.

Identification of OAH specific residues

The enzymes of the isocitrate lyase/PEP mutase enzyme superfamily characterized to date are known to catalyze Mg^{+2} (or Mn^{+2})-dependent C—C bond or P—C bond forming/cleaving reactions, which proceed via α-oxyanion carboxyacid intermediates and/or transition states. The functional subfamilies of enzymes acting on C—C bonds include ketopantoate hydroxymethyl transferase (C—C bond formation), the α-hydroxyacid lyases, isocitrate lyase, 2-methylisocitrate lyase, the plant petal death protein (a nonspecific lyase for C(2) substituted malates and oxaloacetate), and the fungal oxaloacetate acetylhydrolase. The subfamilies of enzymes catalyzing reactions of P—C bonds includes PEP mutase and carboxyPEP mutase, which function in phosphonate biosynthesis, and phosphonopyruvate hydrolase, an enzyme which functions in phosphonate degradation. With the exceptions of the fungal OAH and carboxyPEP mutase, each subfamily is represented by the X-ray structure of one or more liganded enzymes. On the basis of these structures we know that the catalytic scaffold of the isocitratelyase/PEP mutase superfamily is formed at the C-terminal edge of an α/β-barrel by nine peptide segments, one of which is derived from a swapped C-terminal α-helix of an adjacent subunit. The other eight peptide segments are derived from the C-terminal regions of the β-strands, the loops connecting the α and β-elements of

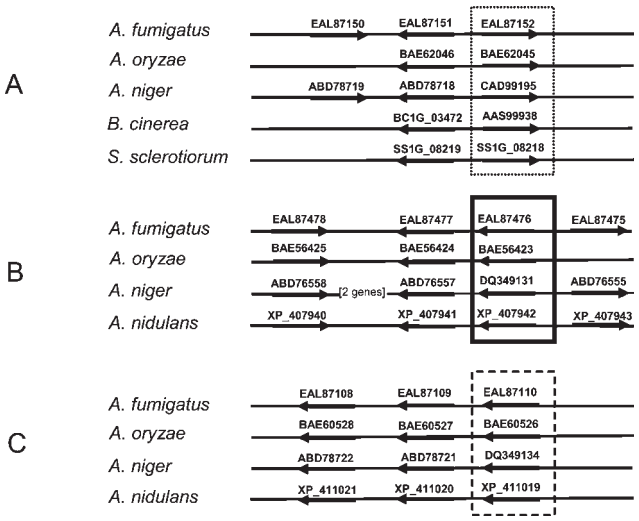

Figure 3

Conservation of synteny between fungal loci encoding OAH-class proteins. Arrows represent genes. Rectangles enclose the OAH-like class protein encoding genes. Dotted borders enclose (putative) OAH. Solid and dashed borders enclose two different orthologous groups of OAH-like class proteins. Encoded protein accession numbers are indicated above the arrows. Panel A: Conservation of synteny at the OAH locus. Panel B and C: Conservation of synteny at loci encoding other OAH-like class proteins.

the barrel, and the N-terminus of a non-barrel helix (see supplementary file for a representation of the superfamily fold). Some residues of the catalytic scaffold are conserved throughout the superfamily (these are core residues used in binding the metal ion cofactor and the substrate α-oxyacid unit) while others vary to form the catalytic machinery tailored for the reaction catalyzed by a particular functional subfamily (these are diversification residues). Our objective was to use the isocitrate lyase/PEP mutase enzyme superfamily 3D-MSA that we had developed to identify an OAH specific residue(s).

Accordingly, the isocitrate lyase/PEP mutase enzyme superfamily 3D-MSA was screened for positions that are more than 90% conserved in the more than 400 unique sequences of the alignment. Matching this query are G34, D41, P58, D62, G66, G68, G84, E91, D92, A115, R116, T117, R127, and D136 (3D-numbering scheme) (Figs. 4 and 5, panel A). Except for A115, which is a glycine in the *C. subvermispora* OAH, these residues are completely conserved in all members of the fungal OAH-like protein class. Many of these positions are located around the active site near the metal ion cofactor and the substrate α-oxyacid group (Fig. 5, panel B). Next, functionally-related diversification residues were identified. This was accomplished by scanning the 3D-MSA for positions that show co-evolution. Residues at positions that show co-evolution tend to be conserved. However, when they do change, a group wise substitution pattern is observed reflecting the different functions of different members. Correlated mutation analysis can reveal these networks of co-evolving positions.[32] Fifteen alignment positions that showed high correlation with at least three other alignment positions were identified (Figs. 4 and 5, panel A). These residues are mainly associated with the region of the catalytic scaffold that houses the substrate moiety that is attached to the α-oxyacid unit. In the isocitrate and 2-methylisocitrate lyases, this region binds the succinyl moiety that is eliminated from the substrate as a result of the C—C bond cleavage. In the petal death protein, this region binds the acetate region that is eliminated from oxaloacetate and from the 2-alkylmalate substrates, and in the organophosphonate metabolizing enzymes this region interacts with the substrate phosphonate substituent.

We then screened the 3D-MSA for positions that are 100% conserved within the known OAHs and at such a position the corresponding amino acid was found in less than 5% of the remaining sequences. This screen resulted in a set of 15 OAH specific residues (Fig. 4). Of these 15 alignment positions only alignment position 157 was also shown to be part of the network of highly correlated positions that separate the different functions present in the superfamily. Alignment position 157 is a serine in all proteins with OAH activity including the petal death protein (S257). Importantly, this serine residue is not found in any of the other OAH-like class proteins. Inspection of the published active site of the petal death protein modeled with (2R, 3S)-2-ethyl-3-methylmalate[31] reveals that the petal death protein S257 (3D-number S157) is directed at the 2-ethyl group. By modeling the gem-diol of oxaloacetate in the active site the petal death protein we found that the pro-R C(2)OH is positioned for deprotonation (which sets off the C—C bond cleavage) and the pro-S C(2)OH (corresponding to the 2-ethyl substituent of the (2R, 3S)-2-ethyl-3-methylmalate ligand), is positioned for hydrogen bond interaction with the S257 side chain. On the basis of the knowledge that oxaloacetate equilibrates with the gem-diol in aqueous solution, and that the petal death protein catalyzes C(2)—C(3) bond cleavage in 2R-alkylmalates, it has been hypothesized that the petal death protein converts oxaloacetate to oxalate and acetate by first binding the gem-diol form of oxaloacetate (a minor component of the equilibrium with the ketone) and then subjecting it to the same catalytic cycle used in lysis of the 2R-alkylmalate substrates.[20] An alternative mechanism involves addition of an active site water molecule at the C(2)=O of the bound oxaloacetate to form the C(2)gem-diol intermediate, followed by C(2)—C(3) bond cleavage. An analogous range of catalytic potential appears to be operative in OAH, as is evidenced by the ability of OAH to catalyze the cleavage (albeit slowly) of (3S, 2R)-2,3-dimethylmalate, in addition the hydrolytic cleavage of oxaloactetate. We have recently found that the C(2) gemdiol of 3,3-difluorooxaloacetate binds to OAH with high affinity,

DOI 10.1002/prot

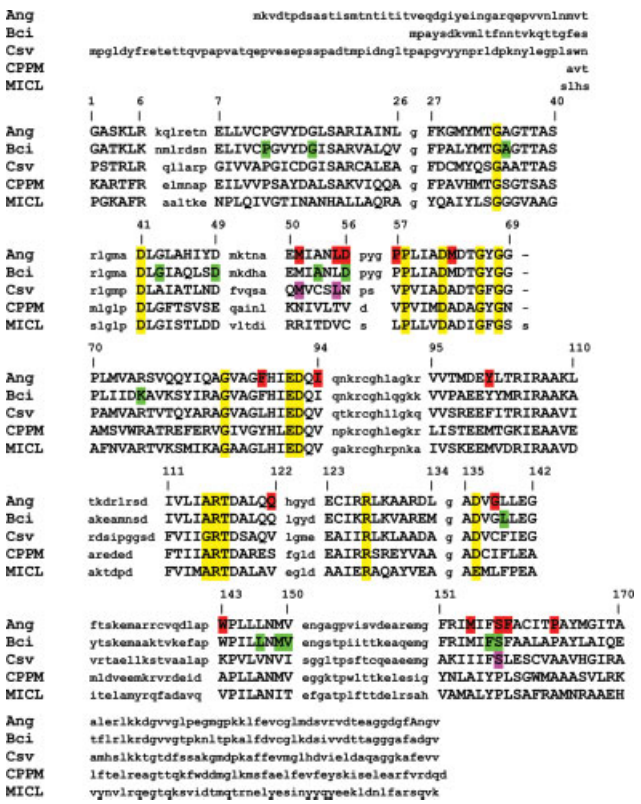

Figure 4

Excerpt of the structure-based multiple sequence alignment of the PEP superfamily. Included in this subset are OAH of A. niger, B. cinerea, *and* C. subvermispora *together with CPPM of S. hygroscopicus and MCIL of* E. coli. *(For accession numbers see Table I) Alignment positions that are structurally conserved within the PEP superfamily are in capitals. Structurally variable parts (lower case, gray) should be considered as not aligned. Positions that are more than 90% conserved within the complete superfamily are highlighted yellow. Alignment positions that highly correlate with at least three other alignment positions are highlighted green and are indicated in the* B. cinerea *sequence. The 15 alignment positions that are 100% conserved within the four ascomycete OAH protein sequences are highlighted red and are indicated in the* A. niger *sequence. These residues are present in less then 5% of the remaining sequences. Of these 15 positions three positions are evolutionary conserved within all in (predicted) OAH sequences; these are highlighted purple in the* C. subvermispora *sequence. Note that only S157 is conserved in all (predicted) OAH proteins and also part of the network of highly correlating positions.*

which is consistent with strong binding interactions between the enzyme active site and the oxaloacetate C(2) gem-diol in the enzyme-substrate complex or in an enzyme-intermediate complex.[21] The conservation of S157 (3D-numbering scheme) among OAH active proteins thus appears to have a functional rather than a structural basis. Namely, S157 might bind the pro-S C(2)OH of the oxaloacetate gem-diol substrate through hydrogen bond formation. This interaction would contribute favorable binding energy for substrate binding and/or catalysis. To test this hypothesis we carried out the mutagenesis study described in the following section.

Evaluation of the S157 OAH sequence marker

The contribution that the active site serine makes in catalysis of the cleavage of oxaloacetate to oxalate and acetate was evaluated in the *B. cinerea* OAH and in the carnation petal death protein. Residues with 3D-number 157 of *B. cinerea* OAH (S260) and of petal death protein

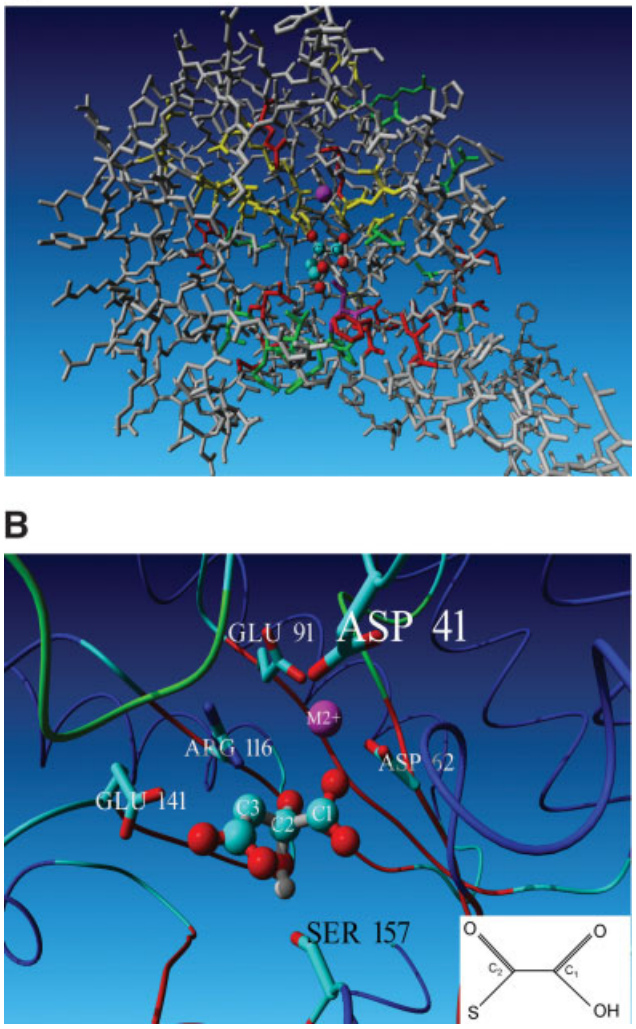

Figure 5

A: Conserved and functionally related diversification residues in the 3D model structure of oxaloacetate hydrolase from Aspergillus niger. *Panel A: Positions that show more then 90% conservation within the PEP superfamily alignment are in yellow. Positions that show a high CMA score are in green. OAH specific residues are in red. Amino acid S157 (in purple) is specific for OAH and shows a high CMA score.* ***B****: Conserved and functionally related diversification residues in the 3D model structure of oxaloacetate hydrolase from* Aspergillus niger. *Panel B: Gem-diol of oxaloacetate modeled in the active site of petal death protein (1ZLP). Side-chains of important active site residues conserved in the superfamily are shown (white label). Ser157 important for OAH activity (black label) is optimally positioned for hydrogen bonding the gem-diol. M2+ indicates the metal ion involved in the catalysis. Insert: The α-keto-acid group, a common backbone of the substrates of the PEP superfamily enzymes.*

Table II
Steady-State Kinetic Constants Determined for OAH and PDP Catalyzed Conversion of Oxaloacetate to Oxalate and Acetate in 5 mM $MgCl_2$ and 0.1M Imidazole Buffer (pH = 7.5, 25°C)

Enzyme	k_{cat} (s^{-1})	K_m (μM)	k_{cat}/K_m (M^{-1} s^{-1})
OAH-WT	17.4 ± 0.2	65 ± 3	2×10^5
OAH-S260T[a]	2.59 ± 0.06	7000 ± 400	4×10^2
OAH-S260T[b]	3.6 ± 0.1	7700 ± 500	5×10^2
OAH-S260A[a]	0.83 ± 0.01	700 ± 30	1×10^3
OAH-S260A[b]	0.71 ± 0.01	1307 ± 60	5×10^2
OAH-S260P[a]	0.96 ± 0.03	150 ± 20	6×10^3
OAH-S260P[b]	0.98 ± 0.03	220 ± 20	5×10^3
PDP-WT	2.72 ± 0.06	130 ± 10	2×10^4
PDP-S257T[a]	1.14 ± 0.02	3600 ± 200	3×10^2
PDP-S257T[b]	1.16 ± 0.03	2600 ± 200	5×10^2
PDP-S257A	2.91 ± 0.07	1530 ± 80	2×10^3
PDP-S257P	4.1 ± 0.1	840 ± 50	5×10^3

[a]Trial 1.
[b]Trial 2.

(S257) were mutated to Ala, Pro and Thr so to replicate the residue usage in the other known isocitrate lyase/PEP mutase family members. The four OAH-like proteins of *A. niger* contain Pro at this position. The effect of the Ser replacement on the kinetic constants for catalysis of oxaloacetate conversion to oxalate and acetate can be seen from inspection of Table II. The k_{cat} decreases by a factor of only 5–20. In contrast the K_m values change more than 100-fold for the S157T mutation. When taking the k_{cat} values into consideration, it is clear that the Ser to Thr replacement is best tolerated. This might be due to the ability of the Thr hydroxyl group to engage in hydrogen bond formation with the C(2)OH of the oxaloacetate gem-diol. On the other hand, the k_{cat}/K_m determined for the Thr mutant is considerably lower than that of the wild-type OAH (∼1000-fold) and the S157A or S157P OAH mutants. The apparent drop in substrate binding affinity is probably attributed to an unfavorable steric interaction introduced by the methyl group of the Thr secondary alcohol. The S157A and S157P mutants display k_{cat} values that are threefold less than that of the S157T mutant and 20-fold less than that of the wild-type OAH. This decrease in k_{cat} values relative to the S157T mutant may be due to the absence of hydrogen bond formation to the Pro-S C(2)OH of the oxaloacetate C(2) gem-diol. However, in contrast to the S157T mutant the substrate binding is less influenced in the S157A and S157P mutant, probably owing to a diminished steric interaction in the latter two relative to the S157T mutant. The k_{cat}/K_m value of the S157A mutant is 300-fold less than that of wild-type OAH, whereas that of the S157P mutant is 50-fold less. On the basis of these results, it is clear that the OAH S157 makes a significant contribution to OAH catalysis.

To determine if S257 (3D-number S157) of the petal death protein also makes a significant contribution to catalysis of oxaloacetate cleavage to oxalate and acetate, it too was replaced with Thr, Ala and Pro. The steady-state kinetic constants measured for oxaloacetate cleavage are listed in Table II; whereas, the k_{cat} value was not significantly altered by the S257 replacements, the k_{cat}/K_m was noticeably decreased: ∼100 fold for the S257T substitution and ∼10-fold for the S257A or S257P substitution. This effect is not as substantial as that observed with OAH, however this is to be expected in view of the fact that the petal death protein active site has evolved to function as a scavenger for C(2) substituted malates. The OAH active site by comparison is specialized in oxaloacetate cleavage. Indeed, not only is the k_{cat}/K_m for oxaloacetate cleavage 10-fold greater than that of the petal death protein, but its substrate specificity is much greater (Table II); whereas the petal death protein can catalyze the cleavage of the 2R-ethyl-3S-methylmalate with the same efficiency as the oxaloacetate, the OAH catalyzed lysis reaction of (2R, 3S) 2,3-dimethlmalate is 100-fold slower than the hydrolytic cleavage of the oxaloacetate (Tables II–IV).

It is a well-known fact among mechanistic enzymologists that the replacement of an enzyme active residue is likely to reduce catalytic efficiency (k_{cat}/K_m), independent of whether the residue directly interacts with the reactant. For this reason, we could not unequivocally conclude that the OAH and petal death active site Ser residues assume the role that we have proposed simply based on reduced activity in the Ser mutants. To arrive at such a conclusion, we needed an internal control to determine whether the Ser substitution had altered the configuration of active site residues. The control experiment was carried out to determine the impact of the Ser mutation on catalysis of C—C bond cleavage in an analogous substrate that lacked the pro S C(2)OH of the oxaloacetate gem-diol. Accordingly, we measured the kinetic constants for wild-type OAH and OAH Ser mutants catalysis of C—C bond cleavage in 3*S*,2*R*-dimethylmalate (the most active substrate following oxaloacetate[23]), and the kinetic constants for wild-type petal death protein and petal death protein Ser mutants catalyzed C—C bond cleavage in 3S-methyl, 2R-ethyl-malate (the most active substrate). The results are shown in Table III and IV, respectively. In contrast to the reduction observed in efficiency of OAH catalysis of oxaloacetate cleavage upon Ser260 (3D-number S157) replacement, the efficiency of

Table III
Steady-State Kinetic Constants Determined for the OAH Catalyzed Conversion of 2R, 3S-2,3-Dimethylmalate to Pyruvate and Propionic Acid in 5 mM $MgCl_2$ and 50 mM HEPES buffer (pH = 7.5, 25°C)

Enzyme	k_{cat} (s^{-1})	K_m (μM)	k_{cat}/K_m (M^{-1} s^{-1})
OAH-WT	0.0293 ± 0.0007	140 ± 10	2×10^2
OAH-S260A	0.0249 ± 0.0002	54 ± 2	5×10^2
OAH-S260P	0.074 ± 0.002	22 ± 2	3×10^3

DOI 10.1002/prot

Table IV
Steady-State Kinetic Constants Determined for the PDP Catalyzed Conversion of 2R-Ethyl-3S-methylmalate to α-Ketobutyrate and Propionic Acid in 5 mM $MgCl_2$ and 50 mM HEPES buffer (pH = 7.5, 25°C)

WT or Mutants	k_{cat} (s^{-1})	K_m (μM)	k_{cat}/K_m (M^{-1} s^{-1})
PDP-WT	8.4 ± 0.1	530 ± 30	2×10^4
PDP-S257A	5.4 ± 0.2	560 ± 50	1×10^4
PDP-S257P	8.3 ± 0.2	660 ± 40	1×10^4

catalysis of C—C bond cleavage in 3*S*,2*R*-dimethylmalate actually improved slightly. In the case of the petal death protein the catalytic efficiency was essentially unchanged, consistent with the comparatively lax substrate specificity exhibited by this particular lyase.

CONCLUSION

The isocitrate lyase/PEP mutase enzyme superfamily is represented in fungal genomes by isocitrate lyase, 2-methylisocitrate lyase and one or more members of the OAH-like class of proteins. In *A. niger* for example the OAH class contains OAH encoded by oahA and two genes encoding enzymes that share 52% sequence identity with the OAH and two genes encoding enzymes that share 34% sequence identity with the OAH. Each of these five enzymes contains catalytic residues that distinguish the C—C bond lyase branch of the family, namely the Cys general base and Glu general acid. Our working hypothesis is that all are in fact C—C bond lyases, however only one is specialized for oxaloacetate cleavage. The specialization derives from a strategically placed serine residue S281 (3D number S157) which functions to bind and orient the minor, hydrated form (gem-diol) of oxaloacetate. Presently, we do not know the exact nature of the catalytic functions performed by the other four enzymes. In each of these sequences a proline occupies alignment position 157, which implies that they are in fact not OAH active enzymes. This is consistent with genetic studies that have demonstrated that oxalate production in *A. niger* is totally dependent on the OAH encoding gene.[12,14,23] In on going work we aim to identify the functions of these four OAH homologs.

The results from our studies are evidence that the following uncharacterized proteins are OAHs: EAL87152 of *A. fumigatus*, BAE62045 of *A. oryzae*, SS1G_08218 of *S. sclerotiorum*, the protein encoded by ORF 7156 of *Phanerochaete chrysosporium*, CC1G_06900.1 of *Coprinus cinereus*, and OAH of *G. trabeum*. It is noteworthy that although basidiomycete fungi are evolutionary very distant from the ascomycete fungi (Fig. 1) the S157 is still conserved and that all known oxalic acid producers posses a predicted OAH encoding gene (Table I) (Fig. 2), consistent with the view that the conversion of oxaloacetate into oxalate and acetate is the main route for oxalic acid biosynthesis in fungi.

REFERENCES

1. Dutton, Evans CS. Oxalate production by fungi: its role in pathogenicity and ecology in the soil enviroment. Can J Microbiol 1996; 42:881–895.
2. Kirkland BH, Eisa A, Keyhani NO. Oxalic acid as a fungal acaracidal virulence factor. J Med Entomol 2005;42:346–351.
3. Maxwell DP, Bateman DF. Oxalic acid biosynthesis by *Sclerotium rolfsii*. Phytopathology 1968;58:1635–1642.
4. Godoy G, Steadman JR, Dickman B, Dam R. Use of mutants to demonstrate the role of oxalic acid in pathogenicity of Sclerotinia sclerotiorum on *Phaseolus vulgaris*. Physiol Mol Plant Pathol 1990; 37:179–191.
5. Nakagawa Y, Shimazu K, Ebihara M, Nakagawa K. *Aspergillus niger* pneumonia with fatal pulmonary oxalosis. J Infect Chemother 1999; 5:97–100.
6. Kubicek CP, Schreferl-Kunar G, Wohrer W, Rohr M. Evidence for a cytoplasmic pathway of oxalate biosynthesis in *Aspergillus niger*. Appl Environ Microbiol 1988;54:633–637.
7. Balmforth AJ, Thomson A. Isolation and characterization of glyoxylate dehydrogenase from the fungus *Sclerotium rolfsii*. Biochem J 1984;218:113–118.
8. Hammel KE, Mozuch MD, Jensen KA. Jr., Kersten PJ. H_2O_2 recycling during oxidation of the arylglycerol beta-aryl ether lignin structure by lignin peroxidase and glyoxal oxidase. Biochemistry 1994;33:13349–13354.
9. Yaver D, Cherry B, Murrell J. Polypeptides having oxaloacetate hydrolase activity and nucleic acids encoding same. US Patent 6,939,701, 2004.
10. Munir E, Yoon Gem JJ, Tokimatsu T, Hattori T, Shimada M. A physiological role for oxalic acid biosynthesis in the wood-rotting basidiomycete *Fomitopsis palustris*. Proc Natl Acad Sci USA 2001;98: 11126–11130.
11. Akamatsu Y, Takahashi M, Shimada M. Influences of various factors on oxaloactase activity of the brown-rot fungus *Tyromyces palustris*. Mokuzia Gakkaishi 1993;39:352–356.
12. Ruijter GJ, van de Vondervoort PJ, Visser J. Oxalic acid production by *Aspergillus niger*: an oxalate-non-producing mutant produces citric acid at pH 5 and in the presence of manganese. J Microbiol 1999;145:2569–2576.
13. Pedersen H, Gem C, Nielsen J. Cloning and characterization of oah, the gene encoding oxaloacetate hydrolase in *Aspergillus niger*. J Mol Gen Genet 2000;263:281–286.
14. Pedersen H, Christensen B, Hjort C, Nielsen J. Construction and characterization of an oxalic acid nonproducing strain of *Aspergillus niger*. Metab Eng 2000;2:34–41.
15. Folkertsma S, van Noort P, Van Durme J, Joosten HJ, Bettler E, Fleuren W, Oliveira L, Horn F, de Vlieg J, Vriend G. A family-based approach reveals the function of residues in the nuclear receptor ligand-binding domain. J Mol Biol 2004;341:321–335.
16. Verhoeff K, Leeman M, Peer R, Posthuma L, Schot N, van Eijk GW. Changes in pH and the production of organic acids during colonisation of tomato petioles by *Botrytis cinerea*. J Phytopathol 1988; 122:327–336.
17. Khabir A, Makni S, Ayadi L, Boudawara T, Frikha I, Sahnoun Y, Jlidi R. Pulmonary oxalosis with necrotizing pulmonary aspergillosis. Ann Pathol 2002;22:121–123.
18. Guimaraes RL, Stotz HU. Oxalate production by Sclerotinia sclerotiorum deregulates guard cells during infection. Plant Physiol 2004; 136:3703–3711.
19. Kenealy WR, Dietrich DM. Growth and fermentation responses of Phanerochaete chrysosporium to O2 limitation. Enzyme Microb Technol 2004;34:490–498.

20. Lu Z, Feng X, Song L, Han Y, Kim A, Herzberg O, Woodson WR, Martin BM, Mariano PS, Dunaway-Mariano D. Diversity of function in the isocitrate lyase enzyme superfamily: the *Dianthus caryophyllus* petal death protein cleaves alpha-keto and alpha-hydroxycarboxylic acids. Biochemistry 2005;44:16365–16376.
21. Han Y, Joosten HJ, Niu W, Zhao Z, Mariano PS, McCalman MT, van Kan JAL, Schaap PJ, Dunaway-Mariano D. Oxaloacetate hydrolase: the C—C bond lyase of oxalate secreting fungi. Submitted.
22. Andreeva A, Howorth D, Brenner SE, Hubbard TJ, Chothia C, Murzin AG. SCOP database in 2004: refinements integrate structure and sequence family data. Nucleic Acids Res 2004:32;226–229.
23. Vriend G. WHAT IF: a molecular modeling and drug design program. J Mol Graph 1990;8:52–56
24. Shulman AI, Larson C, Mangelsdorf DJ, Ranganathan R. Structural determinants of allosteric ligand activation in RXR heterodimers. Cell 2004;116:417–429.
25. Thompson JD, Higgins DG, Gibson TJ. CLUSTAL W: improving the sensitivity of progressive multiple sequence alignment through sequence weighting, position-specific gap penalties and weight matrix choice. Nucleic Acids Res 1994;22:4673–4680.
26. Schmidt HA, Strimmer K, Vingron M, von Haeseler A. TREE-PUZZLE: maximum likelihood phylogenetic analysis using quartets and parallel computing. Bioinformatics 2002;18:502–504.
27. Muller T, Vingron M. Modeling amino acid replacement. J Comput Biol 2000;7:761–776.
28. Howe K, Bateman A, Durbin R. QuickTree: building huge neighbour-joining trees of protein sequences. Bioinformatics 2002;18:1546–1547.
29. Page RD. TreeView: an application to display phylogenetic trees on personal computers. Comput Appl Biosci 1996;12:357–358.
30. Van Durme J, Horn F, Costagliola S, Vriend G, Vassart G. GRIS: Glycoprotein-hormone Receptor Information System. Mol Endocrinol 2006;20:2247–2255.
31. Teplyakov A, Liu S, Lu Z, Howard A, Dunaway-Mariano D, Herzberg O. Crystal structure of the petal death protein from carnation flower. Biochemistry 2005;44:16377–16384.
32. Oliveira L, Paiva CM, Vriend G. Correlated mutation analyses on very large sequence families. Chembiochem 2002;3:1010–1017.

 DOI 10.1002/prot